

Ligand-Dependent Conformational Equilibria of Serum Albumin Revealed by Tryptophan Fluorescence Quenching

Neil Chadborn,* Jason Bryant,# Angus J. Bain,# and Paul O'Shea*

*The School of Pharmacy, Cardiff University, Cardiff CF1 3XF, Wales, and #Department of Physics, University of Essex, Colchester CO4 3SQ, England

ABSTRACT Ligand-dependent structural changes in serum albumin are suggested to underlie its role in physiological solute transport and receptor-mediated cellular selection. Evidence of ligand-induced (oleic acid) structural changes in serum albumin are shown in both time-resolved and steady-state fluorescence quenching and anisotropy measurements of tryptophan 214 (Trp²¹⁴). These studies were augmented with column chromatography separations. It was found that both the steady-state and time-resolved Stern-Volmer collisional quenching studies of Trp²¹⁴ with acrylamide pointed to the existence of an oleate-dependent structural transformation. The bimolecular quenching rate constant of defatted human serum albumin, $1.96 \times 10^9 \text{ M}^{-1} \text{ s}^{-1}$, decreased to $0.94 \times 10^9 \text{ M}^{-1} \text{ s}^{-1}$ after incubation with oleic acid (9:1). Furthermore, Stern-Volmer quenching studies following fractionation of the structural forms by hydrophobic interaction chromatography were in accordance with this interpretation. Time-resolved fluorescence anisotropy measurements of the Trp²¹⁴ residue yielded information of motion within the protein together with the whole protein molecule. Characteristic changes in these motions were observed after the binding of oleate to albumin. The addition of oleate was accompanied by an increase in the rotational diffusion time of the albumin molecule from ~ 22 to 33.6 ns. Within the body of the protein, however, the rotational diffusion time for Trp²¹⁴ exhibited a slight decrease from 191 to 182 ps and was accompanied by a decrease in the extent of the angular motion of Trp²¹⁴, indicating a transition after oleate binding to a more spatially restricted but less viscous environment.

INTRODUCTION

Albumin is the most abundant serum protein and is thought to play many roles in the mammalian circulatory system, of which solute transport is one of the most studied (Peters, 1996). The precise mechanisms of transport and targeting are still unclear but are likely to depend on the nature of the ligand being carried, and there is evidence that albumin may act more specifically by targeting ligands to particular tissues (Peters, 1996; Weiseger et al., 1981). Fatty acids, such as oleic acid, are important examples of such ligands. As their solubilities are low, the majority (99.9%) appear to be carried by albumin (Peters, 1996; Rose et al., 1994; Curry et al., 1998).

The conformational properties of albumin have been investigated for a number of years. Early studies indicated that there may be up to five different pH-dependent conformations possible. The range of pH in these studies, however, might be considered rather far from those that albumin could be exposed to, under any physiological circumstances. Nevertheless, it is possible that more physiologically relevant structural changes in albumin occur during ligand binding (Narazaki et al., 1997). Studies of the dielectric dispersion and macroscopic viscosity of solutions of albumin indicated that the binding of fatty acids to albumin promotes some form of conformational change (Soetewey

et al., 1972). Two of the spatial dimensions of defatted albumin, determined as $34 \times 141 \text{ \AA}$, were found to change on binding of the fatty acid to $40 \times 130 \text{ \AA}$. These transitions may also be related to the observations reported by Bjerrum et al. (1995), who suggest that two conformations of human serum albumin (HSA) exist in a slow equilibrium ($t_{1/2} = 1\frac{1}{4} \text{ h}$), as resolved by hydrophobic interaction chromatography (HIC).

The single tryptophan residue of HSA is located at position 214 in the second α -helix of the second domain (subdomain IIA). From x-ray diffraction studies (Carter and Ho, 1994) this tryptophan residue was found to be located on one side of a binding pocket in this domain. Tryptophan fluorescence has yielded much information about the local environment in a protein and has found extensive application as a probe of protein structure and dynamics (Hochstrasser and Negus, 1984; Ross et al., 1981a,b; Ludescher et al., 1985; Gratton et al., 1986) via lifetime and anisotropy decay measurements. In solution the ground to first excited state transition involves two closely lying singlet states denoted 1L_a and 1L_b (Valeur and Weber, 1977; Callis, 1997) with approximately orthogonal transition dipole moments (Callis, 1997; Yamamoto and Tanaka, 1972). The polarization of tryptophan fluorescence is strongly dependent upon the relative contributions of these two transitions in both the absorption and emission processes. Studies by Valeur and Weber (1977) indicate that in hydrophilic solvents the 1L_a transition predominates at wavelengths above 295 nm. In HSA the presence of multiple tyrosine residues gives rise to an additional absorption route, and although the resulting fluorescence is relatively weak, there is the potential complication of energy transfer to tryptophan. At wavelengths above the 290 nm tyrosine absorption, however, this is minimal and is usually neglected (Lakowicz, 1986).

Received for publication 10 August 1998 and in final form 22 December 1998.

Address reprint requests to Dr. Paul O'Shea, School of Pharmacy, Redwood Building, Cardiff University, King Edward VII Avenue, Cardiff CF1 3XF, Wales. Tel.: 44-1222-875826; Fax: 44-1222-874149; E-mail: osheaps@cardiff.ac.uk.

© 1999 by the Biophysical Society

0006-3495/99/04/2198/10 \$2.00

In addition to the 1L_a and 1L_b electronic states, there is evidence that tryptophan exists in two conformational states. The observation that fluorescence lifetime measurements of free and conjugated tryptophan, in simple peptides, invariably yield double-exponential nanosecond decays has been explained in terms of the presence of two conformations differing in rotation of the $\alpha C-\beta C$ and $\beta C-\gamma C$ bond angles (χ_1 and χ_2) (Fig. 1) (Szabo and Raynor, 1980). These conclusions were further supported by polarization-dependent excitation-lifetime studies of tryptophan in peptide crystals (Dahms et al., 1995).

Picosecond fluorescence anisotropy measurements of tryptophan in serum albumin, in buffer solution (Gentin et al., 1990), water/glycerol (Munro et al., 1979), and propylene glycol at -60°C (Lakowicz and Gryczynski, 1992), all yield "initial" anisotropy measurements well below the value of 0.4 required for parallel absorption and emission dipole moment directions. Evidence from subpicosecond anisotropy measurements of tryptophan in melittin by Fleming and co-workers indicate an internal conversion between 1L_b and 1L_a that occurs on a ~ 1.5 ps time scale (Hansen et al., 1992), in accordance with earlier predictions from molecular dynamic simulations (Ichiye and Karplus, 1983). Picosecond single-photon counting measurements thus yield a reduced "initial" anisotropy as a result of the net averaging of this and equivalently fast depolarization mechanisms (Lakowicz and Gryczynski, 1992).

In the picosecond domain, the first observable decay of anisotropy is interpreted as the diffusive motion of the tryptophan residue within the protein matrix and is found to increase dramatically with temperature between 20°C and 25°C (Munro et al., 1979; Gentin et al., 1990). This suggests that a temperature-dependent conformational change has occurred within the protein structure surrounding the tryptophan residue. Assuming that the diffusion of the tryptophan residue within the protein is limited, the residue will finally adopt a stable conformation in the protein matrix. The remaining decay in anisotropy will then be dependent on the overall rotational diffusion of the protein as a whole. Three studies of the anisotropy decay of serum albumin yield consistent results for the long rotational correlation time, ~ 30 ns (Munro et al., 1979; Gentin et al., 1990;

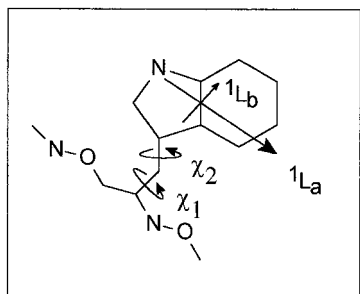


FIGURE 1 From Yamamoto and Tanaka (1972). Directions of 1L_a and 1L_b transition moments in tryptophan side chain, determined from polarized absorption spectra.

Lakowicz and Gryczynski, 1992). Calculating the theoretical rotational diffusion constant from the Stokes-Einstein-Debye equation, assuming the protein is spherical, results in a similar value and is consistent with measurements by dielectric relaxation (Soetewey et al., 1972). Observation of a change in this correlation time in a given solvent environment may indicate a change in either the hydrodynamic volume or shape of the protein.

Albumin has been found to bind to specific cell surface receptors. These have been identified on endothelial cells and hepatocytes (Peters, 1996) and blood cells (Wall et al., 1995). It seems likely, therefore, that cellular receptors recognize and preferentially bind albumin molecules carrying certain ligands (or deligated albumin), in a manner similar to that of the advanced glycation end-product or scavenger receptor, which recognizes glycated albumins (Peters, 1996). A ligand-dependent conformational change of the albumin molecule may underlie the mechanism of recognition; thus identification of ligand-dependent conformational changes will aid the understanding of the molecular basis of the systemic physiology of albumin.

With these reports in mind, in the present study we have exploited the fact that HSA possesses a single tryptophan (Trp^{214}). It is feasible, therefore, to study the accessibility of this moiety by collisional fluorescence quenching. Tryptophan quenching in HSA and related proteins has been studied using a number of quenching agents (Lakowicz and Weber, 1973; Eftink and Ghiron, 1976, 1977). In the present study, a Stern-Volmer quenching analysis using acrylamide indicates structural transitions induced by physiological ligand binding to albumin. These observations are related more directly to global structural transitions by the use of protein separation methods. In addition, fluorescence anisotropy time-resolved decay measurements of HSA revealed changes in the local motion of Trp^{214} together with the overall motion of the albumin.

MATERIALS AND METHODS

HSA was obtained from Armour Pharmaceuticals, either as defatted or with bound fatty acids. HSA was defatted with activated charcoal at low pH (Chen, 1967). Oleic acid, D-tryptophan, and acrylamide (30% solution) were obtained from Sigma. Phenyl sepharose HIC beads (CL-4B) were purchased from Pharmacia.

HSA-oleate complex was prepared by mixing a 9:1 molar ratio of oleic acid (1 M in ethanol) with the albumin. The mixture was then gently agitated for 1 h at room temperature. To measure the rate of binding, acrylamide (final concentration 16 mM) was added to the protein in a stirred cuvette. Three microliters of oleic acid in ethanol was added (final ethanol concentration was below 0.1% v/v), and the fluorescence was measured every 60 s. Between measurements the shutter was closed to avoid photobleaching.

Steady-state fluorescence quenching

Fluorescence emission intensities at 345 nm were measured over 10 s with excitation at 295 nm and averaged. Quenching data were analyzed by the Stern-Volmer equation (Lakowicz, 1986):

$$\frac{F_0}{F} - 1 = K_{SV}Q \quad (1)$$

where F_0 and F are the fluorescence intensities before and after the addition of quencher (concentration Q). K_{sv} is the effective quenching constant and is dependent on both the lifetime before the addition of quencher (τ_0) and the bimolecular rate constant of the quenching reaction (k_q):

$$K_{sv} = k_q \tau_0 \quad (2)$$

Fluorescence lifetime and anisotropy measurements

Fluorescence lifetime and anisotropy decay measurements were performed using a cw mode-locked Nd:YAG pumped, cavity dumped dye laser (Coherent Antares 76-S and 7220D) running with rhodamine-6G and frequency doubled in β -barium borate (Photox). This provided a 4-MHz train of ~ 7 ps pulses at 297 nm, which was used to excite the tryptophan $S_1 \leftarrow S_0$ transition in the albumin samples ($\sim 10 \mu\text{M}$), using a collinear excitation-detection arrangement (Bain et al., 1996). In isotropic media the cylindrical symmetry of the excitation process with respect to the (vertical) laser polarization vector ensures the equivalence of colinear and right-angled excitation-detection geometries (Bain and McCaffery, 1984). Fluorescence was filtered through a 70 nm bandpass interference filter centered at 400 nm (Corion P70-400). Polarization analysis of the emission was undertaken using a computer controlled analyzing polarizer which was used to resolve the vertical, horizontal, and "magic angle" polarization components of the emission. The time evolution of each component was built up using standard time-correlated single photon counting (TCSPC) methods (O'Connor and Phillips, 1984).

In excitation from an isotropic sample (assuming an ultrashort excitation pulse), the relationship between the fluorescence intensity detected at an analyzer angle of β with respect to the excitation polarization direction is given by

$$I(t, \beta) \propto N(t)[1 + (3 \cos^2 \beta - 1)R(t)] \quad (3)$$

where $R(t)$ is the degree of alignment of the emitting transition dipole moment in the laboratory frame and $N(t)$ is the excited state population. For an analyzer angle of $\beta = 54.7^\circ$ (the "magic angle"), the dipole alignment contribution to the emission intensity vanishes, yielding

$$I(t, \beta = 54.7^\circ) \propto N(t) \quad (4)$$

The experimentally determined fluorescence anisotropy is defined by

$$R(t) = \frac{I(t, \beta = 0^\circ) - I(t, \beta = 90^\circ)}{I(t, \beta = 0^\circ) + 2I(t, \beta = 90^\circ)} \quad (5)$$

which is a direct measure of the time-dependent alignment of the emission transition dipoles of the fluorescing population.

As discussed above, TCSPC anisotropy measurements are not sensitive to the fast depolarization mechanisms and yield an initial anisotropy that reflects the averaging of these processes. For tryptophan in HSA, the observed anisotropy should yield double-exponential decays consistent with the evolution of two independent diffusive motions with a significant separation in their respective correlation times according to

$$R(t) = \exp\left(-\frac{t}{t_2}\right) \times \left(A_1 \exp\left(-\frac{t}{t_1}\right) + A_2\right) \quad (6)$$

$$= \left(A_1 \exp\left(-\frac{t}{t_1}\right) + A_2 \exp\left(-\frac{t}{t_2}\right)\right), \quad (t_2 \gg t_1)$$

Isotropic rotational diffusion of the protein corresponds to the slow correlation time t_2 . Restricted rotational diffusion of the tryptophan residue within the protein is represented by an exponential decay to a constant value A_2 with a faster correlation time t_1 . The initial fluorescence anisotropy

therefore corresponds to the sum of A_1 and A_2 . The ratio of A_1 to A_2 , however, is determined by the degree of orientational averaging within the protein matrix; this has been interpreted in terms of diffusion within a cone of semiangle α , which is related to the amplitude of the two decay rates by (Kinosita et al., 1977; Ameloot et al., 1984)

$$A_2/(A_1 + A_2) = \left[\frac{\cos \alpha(1 + \cos \alpha)}{2}\right]^2 \quad (7)$$

Fluorescence lifetimes ($I(t, \beta = 54.7^\circ$) measurements) were analyzed using a standard deconvolution procedure and the response of the apparatus to scattered pump light (Hochstrasser and Negus, 1984; Janes et al., 1987). Experimentally determined fluorescence anisotropies (Eq. 5) were analyzed without deconvolution, using a least-squares fit of the form (Munro et al., 1979; Bain et al., 1998)

$$R(t) = \sum_i A_i \exp\left(-\frac{t}{t_i}\right) \quad (8)$$

Gel filtration chromatography

Gel filtration was carried out on a Sephacryl S300 column equilibrated in 10 mM phosphate-buffered saline. HSA was loaded and eluted at a flow rate of 30 ml/h. Absorbances at 235 and 280 nm were measured. Peaks were pooled and diluted in the same buffer to give approximately equal final concentrations.

Hydrophobic interaction chromatography

For HIC, a 1.2-cm³ column of CL-4B was equilibrated with 0.1 M glycine and 0.038 M Tris-HCl (pH 8.7). The HSA solution was then added and eluted at 5 ml/h. One-milliliter samples were collected, and their absorbance at 280 nm was measured. The elution buffer was substituted for water after the first protein fraction was collected. The fraction eluted in glycine was then diluted with water, and the water fraction was diluted with glycine, so that all samples were in identical media.

RESULTS

Quenching of HSA tryptophan fluorescence by acrylamide and iodide

It is shown in Fig. 2 that the fluorescence of HSA-Trp²¹⁴ may be quenched by iodide or acrylamide, in a manner similar to that of free tryptophan in an aqueous solution. Acrylamide quenching yields a linear Stern-Volmer plot (Eq. 1), which implies that the fluorescence quenching takes place on a simple collisional basis.

The effects of the quenchers on the fluorescence lifetimes were also measured as shown in Fig. 3. The excited-state relaxation was measured using TCSPC, which was best described by a double-exponential function, $\tau_1 = 2.57$ ns, $\tau_2 = 6.87$ ns. From Fig. 3 *A* it is clear that both lifetimes are quenched. Fig. 3 *B* shows that τ_1 , the shorter lifetime, is quenched with a larger Stern-Volmer constant ($K_{sv} = 13.6 (\pm 1.7) \text{ M}^{-1}$) than the longer lifetime, τ_2 ($K_{sv} = 3.1 (\pm 0.5) \text{ M}^{-1}$). The steady-state constant ($K_{sv} = 10.4 (\pm 0.3) \text{ M}^{-1}$) lies between these two values, which is consistent with the interpretation that the steady state is due to collisional quenching. Eftink and Ghiron (1976, 1977), however, suggest that there is a small contribution to the overall quench-

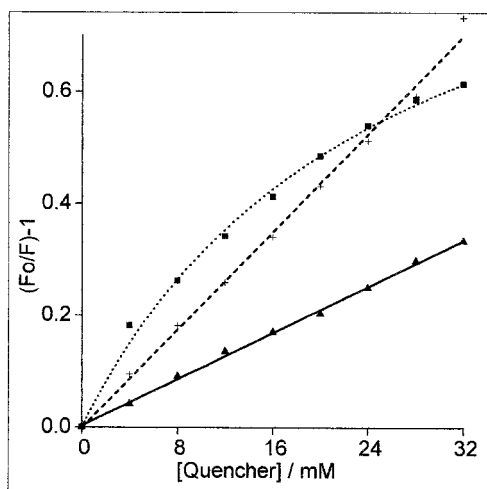


FIGURE 2 Stern-Volmer quenching of HSA and tryptophan. Three milliliters of 10 μ M defatted HSA in 10 mM phosphate-buffered saline (PBS) was excited at 295 nm in a temperature-controlled cuvette (20°C). Emission at 345 nm was collected for 10 s. Serial additions of 6 μ l of 2 M acrylamide, also in PBS, were added, and fluorescence was measured after mixing by inversion (▲). This was repeated for quenching of tryptophan (+) and for iodide quenching of HSA (■).

ing process from static quenching. Such a process was not apparent at the lower quencher concentrations utilized in the present study.

HSA was found to possess a much smaller Stern-Volmer quenching constant than free tryptophan. The corresponding values shown in Fig. 2 were calculated as $10.4 (\pm 0.3)$ and $22.0 (\pm 0.5) \text{ M}^{-1}$, respectively. To compare directly the accessibility of the fluorophores to the quencher according to Eq. 2, the initial lifetime must also be taken into account. Using an amplitude-weighted average of the initial lifetimes from the time-resolved fluorescence (5.3 ns), the bimolecular rate constant (k_q) was calculated to be $1.96 \times 10^9 \text{ M}^{-1} \text{ s}^{-1}$, which is much lower than that previously reported (Eftink and Ghiron, 1977) for free tryptophan ($6.5 \times 10^9 \text{ M}^{-1} \text{ s}^{-1}$). The lower accessibility of acrylamide to Trp^{214} , compared to that of free tryptophan in water, indicates that Trp^{214} is located within the protein matrix of HSA.

The quenching of HSA by iodide is more complicated, as it yields a nonlinear (i.e., positively curved) quenching relation, which is inconsistent with the simple collision-based Stern-Volmer equation (Eqs. 1 and 2). Lehrer (1971) proposed that this was due to the iodide ion binding to HSA. Once bound, iodide may quench the Trp residue in a collisional fashion, by rapid movements within the protein. Thus, in the initial part of the titration curve (i.e., at low iodide concentrations), quenching increases rapidly as iodide binds, but when the site is saturated, quenching is due solely to free iodide in the bulk solvent. Similar complications are clearly present in the observations shown in Fig. 2 and are consistent with Lehrer's proposition. Thus, to avoid these complications in more detailed studies, acrylamide was used as the sole quenching agent.

The effect of oleate on the Trp^{214} fluorescence quenching of HSA by acrylamide

The noncovalent binding of oleate to HSA (Peters, 1996) is shown, in Fig. 4 B, to promote an emission shift from 345 to 333 nm of Trp^{214} , concurrent with a slight increase in quantum yield. Such changes are characteristic of a decrease in the polarity of the environment of Trp (Lakowicz, 1986). A Stern-Volmer analysis of the acrylamide-dependent quenching of the oleate-HSA complex shown in Fig. 4 A yields a much lower value for K_{sv} ($4.4 (\pm 0.3) \text{ M}^{-1}$, measured at the peak wavelength, 333 nm) compared to that of the HSA ($10.6 (\pm 0.2) \text{ M}^{-1}$, measured at 345 nm). The bimolecular quenching constant has decreased from $1.96 \times 10^9 \text{ M}^{-1} \text{ s}^{-1}$ to $0.94 \times 10^9 \text{ M}^{-1} \text{ s}^{-1}$, indicating that in addition to a change in the polar nature of the environment of the tryptophan residue, it has also become less accessible. Fig. 4 B also indicates that quenching by acrylamide does not change the position of the emission peak. Thus acrylamide does not appear to cause any structural changes in the protein, e.g., by nonquenching linked binding.

Binding of oleate to HSA (9:1), as shown in Fig. 3 A, causes a reduction in the lifetimes of the tryptophan residue ($\tau_1 = 1.92 \text{ ns}$, $\tau_2 = 5.75 \text{ ns}$). Stern-Volmer analysis of these two lifetimes reveals a pattern similar to that of the defatted HSA, where the K_{sv} of τ_1 ($6.6 (\pm 0.7) \text{ M}^{-1}$) is slightly higher than the K_{sv} for the steady-state fluorescence, and the K_{sv} of τ_2 ($1.4 (\pm 0.2) \text{ M}^{-1}$) is slightly lower.

Binding sites have been found on each of the three domains of albumin (Peters, 1996). However, from the crystal structure of myristoylate-HSA, the fatty acid binding site of the domain containing Trp^{214} is located on the opposite side of the domain, at a distance of 17 Å. The closest binding site is located in domain III, at a distance of 10 Å (Curry et al., 1998). This suggests that changes revealed by the emission spectra, as well as the quenching data, are not due to direct interactions between the oleate moiety on Trp^{214} , but instead are likely to be caused by a change in the conformation of the HSA after binding oleate, resulting in an altered environment of Trp^{214} .

Kinetics of oleate-dependent fluorescence changes of HSA

Oleate has been observed to promote a decrease in the Stern-Volmer quenching constant (Fig. 4 A), and such experiments are typically performed by adding the quenching agents to the fluorophore, allowing the establishment of equilibrium, and then recording the level of fluorescence. On the other hand, if oleate is added to albumin already in the presence of the quencher, changes in fluorescence intensity would be anticipated to indicate changes in the quenching constant. This phenomenon was indeed observed and illustrated in Fig. 5. These data were found to be best described by a single exponential process, with a rate constant of $8.0 (\pm 1.4) \times 10^{-4} \text{ s}^{-1}$. The rate of change in quenching may arise as a direct influence of the presence of

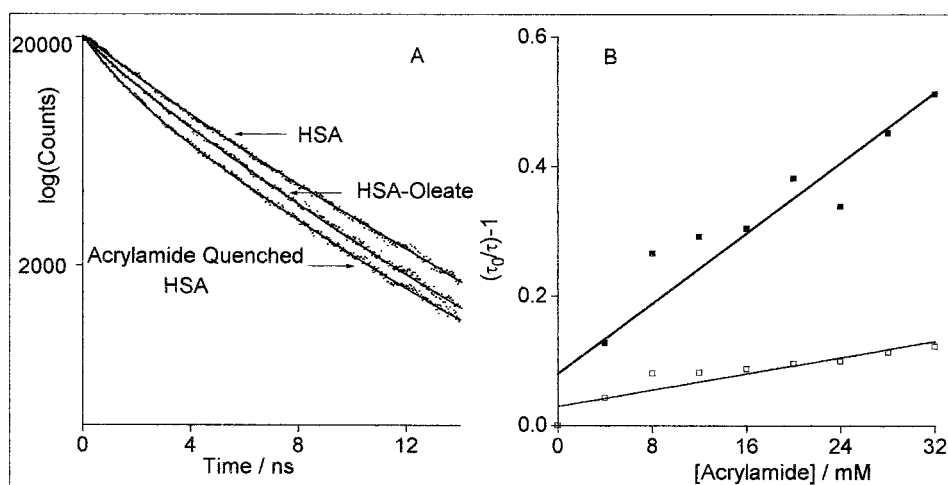


FIGURE 3 (A) TCSPC fluorescence of HSA, HSA-oleate, and acrylamide-quenched HSA. Defatted HSA (10 μ M) in 10 mM PBS was excited at 297 nm with 4-MHz pulses by the frequency-doubled output from a cw mode-locked Nd:YAG pumped cavity dumped rhodamine-6-G dye laser. The tryptophan emission polarized at 54.7° to the excitation polarization was passed through a 70-nm bandpass interference filter centered at 400 nm before reaching the TCSPC microchannel plate photomultiplier. This arrangement ensures there is no orientational contribution to the fluorescent signal and that the observed decays arise purely from population kinetics. This was repeated for HSA incubated for at least 3 h previously with 9:1 oleate and for HSA after the addition of 96 mM acrylamide. (B) Acrylamide quenching of the two lifetime components of HSA as determined by TCSPC. ■, Short lifetime (τ_1). □, Long lifetime (τ_2). Fluorescence lifetimes of HSA were measured as before. Serial additions of 6 μ l of 2 M acrylamide were made and mixed by inversion.

foleate, or as a result of conformational changes induced after oleate binding, which may occur immediately or subsequently much more slowly. The rate constant for the binding of oleate to HSA is reported to be on the order of 3.2 s^{-1} (Scheider, 1980). In view of the fact that this value is about three orders of magnitude larger than that found from the present quenching study (Fig. 5), the most likely explanation of the observed change in quenching is that it reflects a slow conformational change subsequent to the rapid binding step.

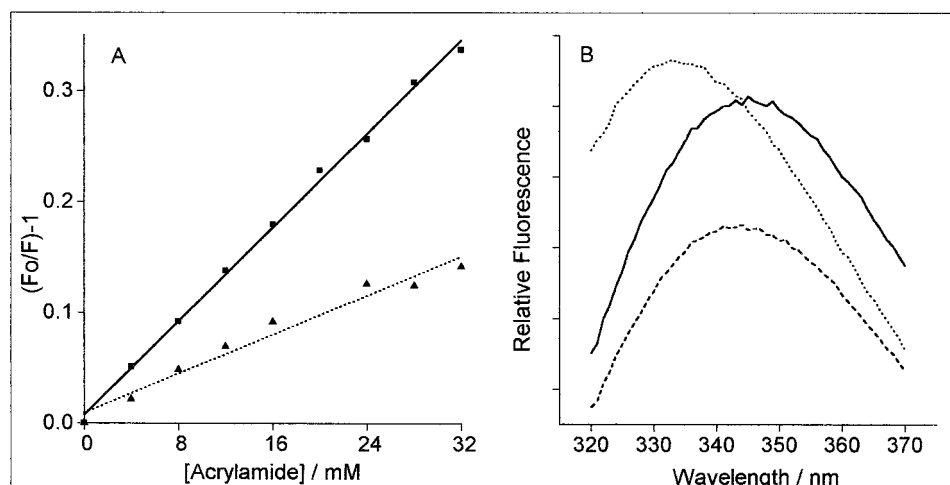
Gel filtration chromatography and hydrophobic interaction chromatography of HSA and oleate-bound HSA

It has been suggested above that albumin undergoes structural changes due to the binding of oleate, which may

undergo slow transformations. In the following section, we describe attempts to isolate such structural conformers. Initially gel filtration techniques were employed to separate dimeric and monomeric forms of albumin to determine whether their Trp fluorescence properties were different.

Treatment of albumin by gel filtration, as shown in Fig. 6, indicates that HSA monomers and dimers may be clearly separated. In Fig. 6 A it can be seen that HSA elutes as two major peaks. The first and smaller peak represents the dimer, whereas the second and larger peak represents the monomer of the protein which, is consistent with earlier reports (Janatova et al., 1968). The elution profile was fitted to a double Gaussian curve, where the area under the curve is proportional to the amount of that fraction present. This analysis revealed that the monomer contributed $92.8 (\pm 3)\%$ of the original sample. This indicates that this albumin

FIGURE 4 (A) Acrylamide quenching of HSA-oleate (▲) compared to control HSA (■). HSA and HSA incubated with 9:1 oleate for at least 3 h were analyzed by Stern-Volmer quenching as in Fig. 2. (B) Emission spectra of HSA (—), acrylamide-quenched HSA (---), and acrylamide-quenched HSA-oleate (.....). Excitation was at 295 nm. The HSA concentration was 10 μ M, with either 32 mM acrylamide or both 32 mM acrylamide and 9:1 oleate.



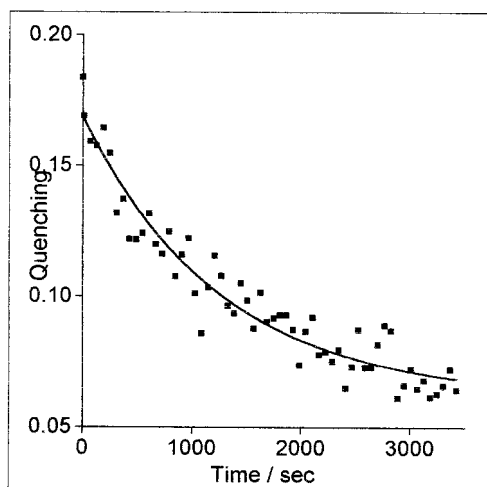


FIGURE 5 Reduction in quenching with time after the addition of oleate (9:1). Acrylamide (32 mM) was added to 10 μ M HSA in PBS. Oleate (2.5 μ l of 90 mM) in ethanol was added, and fluorescence was measured at 345 nm (excitation 295 nm) at 1-min intervals for 1 h. Between measurements the shutter was closed to minimize photobleaching. A control experiment revealed that photobleaching was negligible.

preparation exists predominantly as a monomer. The elution profile of the HSA-oleate complex (monomer = $89.8 (\pm 0.8)\%$) appears virtually identical to that found for the defatted HSA and implies that the binding of oleate does not significantly affect the equilibrium between the populations of monomers and dimers.

A Stern-Volmer quenching analysis with acrylamide (Fig. 6 B) of these separate structural forms of albumin indicates that the monomeric and dimeric forms possess quenching constants of $K_{sv} = 8.6 (\pm 0.1)$ and $6.9 (\pm 0.1)$ M^{-1} , respectively. The small difference in these values indicates that the dimer exhibits a slightly reduced accessibility of the tryptophan to acrylamide. One explanation of this may be that the tryptophan is located at the interface of the dimer components, resulting in a small decrease in exposure to solvent.

The Stern-Volmer quenching constants of the monomeric and dimeric forms of HSA with oleate bound were found to be the same ($K_{sv} = 4 (\pm 0.1)$ M^{-1}) but are much lower than either fraction without oleate. This indicates that oleate may bind to both the monomeric and dimeric forms of HSA, and the consequent change in conformation results in the tryptophan residues of both structural forms becoming equally inaccessible. This quenching constant was found to be equal to that of the unseparated HSA-oleate (Fig. 2 A).

The monomeric and dimeric forms of HSA possess quite different long rotational correlation times (t_2) of 22 and 65 ns, respectively. This may be anticipated, given the differences in size of the molecular units (Fig. 8 B).

HIC was used to separate the different putative conformations of albumin (Bjerrum et al., 1995). Hydrophobic species may bind to the column in the higher ionic strength buffer and may be eluted by the subsequent reduction in

ionic strength. The elution profile of HSA (Fig. 7 A) shows two major peaks. Similar experiments led Bjerrum et al. (1995) to propose that these two fractions are different conformations of albumin, which reequilibrate slowly after separation.

Fig. 7 B indicates a Stern-Volmer analysis of column peak fractions after elution with glycine and water. The quenching constant of the glycine fraction ($K_{sv} = 15 (\pm 0.2)$ M^{-1}) is larger than the water fraction ($K_{sv} = 6.4 (\pm 0.1)$ M^{-1}). On this basis, the Trp²¹⁴ of the albumin eluted in each fraction possesses different accessibilities to acrylamide. This is consistent with the foregoing proposal that the albumin in each fraction exists in a different conformation. The quenching of the defatted HSA, before HIC treatment, has a quenching constant ($K_{sv} = 10.9 (\pm 0.3)$ M^{-1}) between those of the fractionated samples. The emission spectra of the HIC fractions show similar differences. The peaks of the two fractions are shifted to either side of the control, at 348 and 339 nm for HSA in the glycine and water fractions, respectively. This suggests that Trp²¹⁴ of the glycine-eluted HSA exists in a more polar environment than that eluted in the water fraction.

Fig. 7 A shows that after the fractionation of defatted-HSA with HIC, the two major peaks have approximately equal areas, whereas preincubation of HSA with oleate leads to a large increase in the glycine peak area and an equivalent decrease in the water peak. These observations indicate that binding of oleate reduces the affinity of the albumin for the HIC column. One explanation of this is that oleate binds to the same site as the column-linked hydrophobic groups; thus binding is reduced in a competitive manner.

After separation of HSA-oleate (Fig. 7 A) the albumin eluted in the glycine fraction has a reduced K_{sv} ($9 (\pm 0.2)$ M^{-1}), but the water-eluted fraction was found to be unchanged. The emission spectra of the two fractions both show a blue shift, indicating that oleate is bound to both fractions. Presumably it is the binding of oleate that results in the decrease in the K_{sv} of the glycine fraction. The water fraction is unchanged in this respect, however, suggesting that the conformation of the defatted albumin separated in the water fraction is similar to that caused by binding oleate. It may be expected that if oleate binding does result in HSA taking up a conformation similar to that in the water fraction, more of the HSA-oleate complex would bind, increasing the size of the water fraction. The opposite effect was observed experimentally, indicating that oleate competes with the HIC column for a hydrophobic site(s) on the albumin.

Effects of oleate on the time-resolved fluorescence anisotropy of HSA

The fluorescence anisotropy decay for HSA, in phosphate-buffered saline at 20°C, shown in Fig. 8, is characterized by

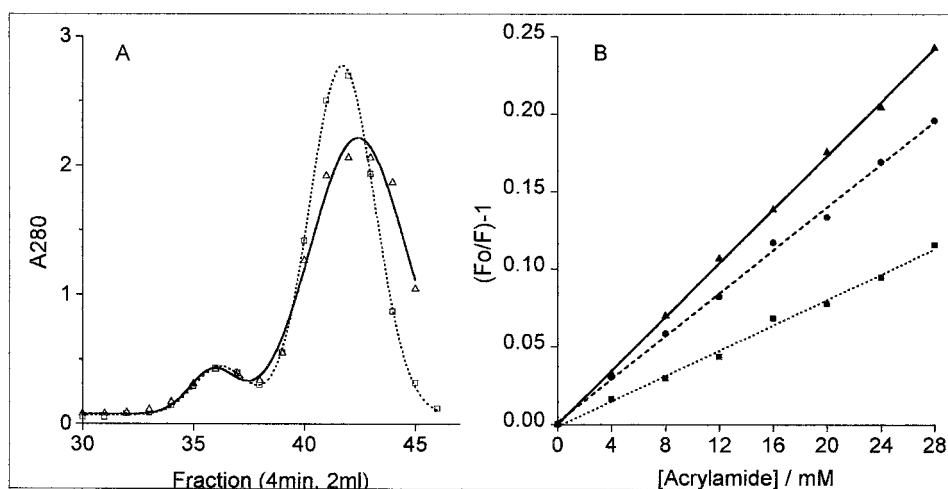


FIGURE 6 (A) Gel filtration. A Sephacryl S300 column was equilibrated in PBS. Defatted HSA was added to the column and eluted at a flow rate of 30 ml/h. Absorbance at 280 nm was used to estimate protein concentration. The elution profile was then fitted to a double Gaussian curve (—). This was repeated for HSA preincubated with 9:1 oleate for at least 3 h (.....). (B) Stern-Volmer analysis of gel filtration fractions. The peak fractions of the above were pooled, and the monomer was diluted in PBS to the same concentration as the dimer. Quenching with acrylamide was then carried out as in Fig. 2. ▲, Defatted monomer; ●, defatted dimer; ■, oleate-bound monomer (equivalent to oleate-bound dimer).

two distinct correlation times, as predicted by Eq. 6 and shown in Table 1 together with the corresponding values for the HSA-oleate complex. The HSA-oleate values are in agreement with previous studies of HSA with native fatty acids bound (Munro et al., 1979; Gentin et al., 1990; Lakowicz and Gryczynski, 1992). The addition of oleate has a significant effect on the anisotropy decay (Fig. 8), indicating changes in the overall rotational diffusion as well as an apparent change in the local environmental viscosity. The correlation time associated with the diffusion of the albumin (t_2) is seen to increase from 22.0 to 33.6 ns, whereas the

internal diffusion time (t_1) of the tryptophan shows a small decrease from 191 to 182 ps. The increased albumin diffusion time (t_2) lies below the value of 65 ns we have measured for the dimeric form of HSA; this is compatible with either an increase in volume or an appropriate change in shape of the albumin as a consequence of the addition of oleate. The change in the internal tryptophan dynamics is potentially more complex, and the decrease in the cone semiangle from 20.8 to 16.1° (and hence an increase in the local order within the protein domain) implies a more restricted local environment for the tryptophan.

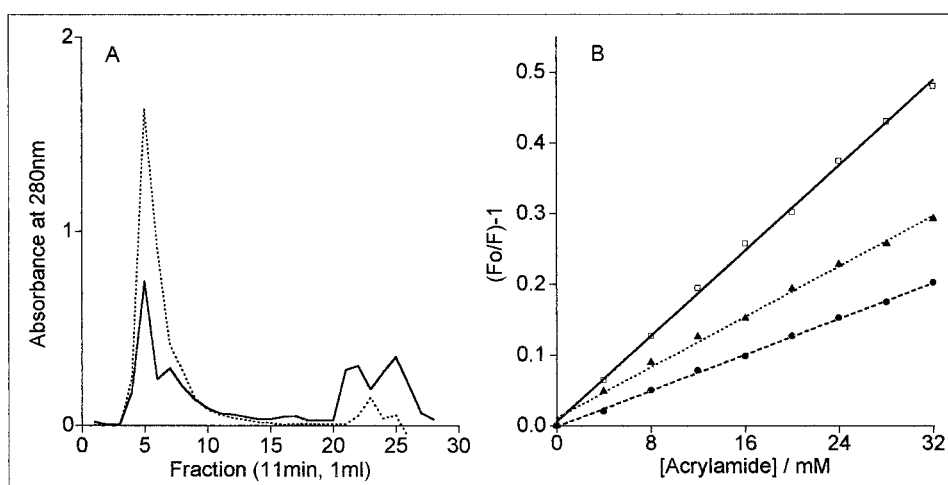


FIGURE 7 (A) Elution profile of HIC of HSA (—) and HSA-oleate (.....). A 1.2-ml column of phenyl Sepharose (CL 4B) was equilibrated in glycine buffer (0.1 M glycine, 0.038 M Tris-HCl, pH 8.7), to which HSA in glycine buffer was added. Elution was at 5 ml/h. After the first peak was collected, the column was eluted with water. The fraction eluted in the glycine buffer was then diluted with water, and vice versa with the water fraction, so that samples were in identical media. This was repeated for HSA incubated with 9:1 oleate. (B) Stern-Volmer quenching with acrylamide of glycine □, water ●, fractions of HSA, and glycine fraction of HSA-oleate ▲ (water fractions of defatted and oleate-HSA were equivalent). Within 30 min of elution from the HIC column, the pooled peaks were analyzed by Stern-Volmer quenching as in Fig. 2.

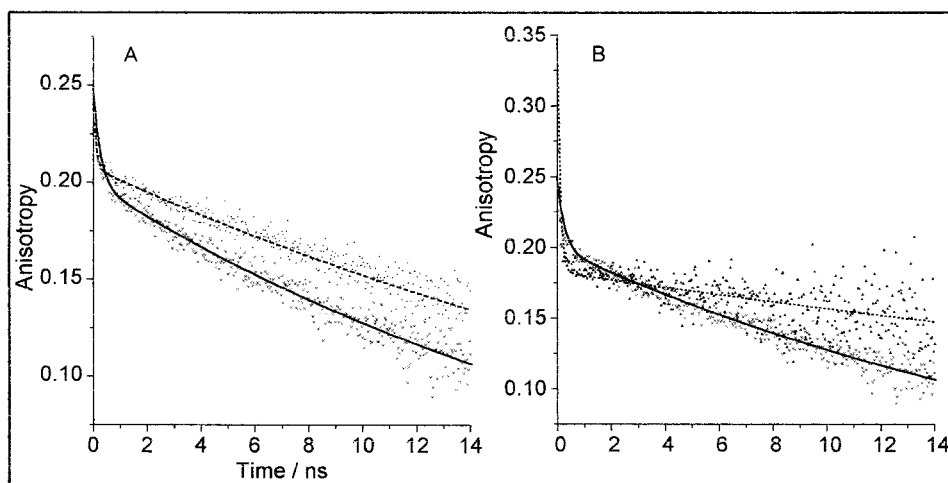


FIGURE 8 TCSPC anisotropy. (A) HSA (—) and HSA-oleate (9:1) (---). Monomeric defatted HSA ($10 \mu\text{M}$) in 10 mM PBS was excited at 297 nm with 4-MHz pulses by the frequency-doubled output from a cw mode-locked Nd:YAG pumped cavity dumped rhodamine-6-G dye laser. The tryptophan emission, polarized parallel (vertical) and perpendicular (horizontal) to the plane of the incident light, was passed through a 70-nm bandpass interference filter centered at 400 nm before it reached the TCSPC microchannel plate photomultiplier. These two polarizations were collected alternately for short periods (~ 10 s), and the whole averaging process lasted for ~ 20 min. This was repeated for HSA previously incubated for at least 3 h with 9:1 oleate. (B) Dimeric HSA (.....) is compared with the monomeric HSA as in A.

DISCUSSION

The binding of oleate causes changes in the environment of the single tryptophan in HSA. The emission spectra show a change in peak position, indicating a decrease in the polarity of the local environment. Stern-Volmer quenching with acrylamide also shows a change in the surroundings of Trp^{214} : the accessibility decreases after oleate binding. These data are supported by the quenching of fluorescent lifetimes of Trp^{214} , which show a similar decrease in quenching constant after oleate binding. From the average of the initial lifetimes it is also possible to calculate the bimolecular rate for acrylamide quenching HSA and HSA-oleate as $1.96 \times 10^9 \text{ M}^{-1} \text{ s}^{-1}$ and $0.94 \times 10^9 \text{ M}^{-1} \text{ s}^{-1}$, respectively. This suggests that the structure of the protein matrix surrounding Trp^{214} has become more compact or denser, thus retarding the diffusion of acrylamide.

This change in the local environment of Trp^{214} is also reflected in the fluorescence anisotropy decay. The semi-angle of the cone through which the tryptophan can diffuse inside the protein decreases from 20.8° to 16.1° after the noncovalent binding of oleate to HSA. This also indicates that the local environment of Trp^{214} has become denser or more compact.

The anisotropy data also reveal a large-scale change in the protein as a whole. The long correlation time (t_2) shows

an increase after the addition of oleate. This indicates that the rotational diffusion of the protein has decreased. The simplest explanation of this is that the size of the protein has increased. This may be due to an increase in hydrodynamic volume or may indicate a shape change of the protein. These changes, however, are not substantial enough to be resolved by gel filtration. It is also worth emphasizing that the monomer/dimer ratio of an HSA solution revealed by gel filtration is not altered by the presence of oleate. On the other hand, dielectric relaxation studies (Soetewey et al., 1972) indicate that binding of oleate results in an increase in the short axis of the protein, when modeled as a prolate ellipsoid, which is consistent with our latter explanation outlined above.

HIC appears to perturb the structure of HSA, resulting in two populations of different conformations. This conformational change affects the local environment of Trp^{214} , because the Stern-Volmer quenching of the two populations indicate different accessibilities to acrylamide. From the quenching constants, the first population appears to be similar to the native HSA, whereas the second population, which has been retarded by the gel, exhibits a reduced quenching constant, the value of which is similar to that of the HSA-oleate, indicating a similar local environment of the Trp^{214} .

Binding of oleate changes the elution profile of HIC. The size of the first peak is increased, and there is a similar decrease in the second peak. This suggests that the oleate is competing for the binding site of the protein. The Stern-Volmer quenching constant of the first peak is reduced, indicating that oleate is bound. Although the emission spectrum of the second peak indicates that oleate is bound, the quenching constant is unchanged. This implies that the

TABLE 1 Analysis of the anisotropy decays according to Eq. 6, yielding correlation times t_1 and t_2 and amplitudes A_1 and A_2

Sample	t_1 (ns)	A_1	t_2 (ns)	A_2
HSA	0.191	0.044	22.2	0.199
HSA-oleic	0.182	0.026	33.6	0.207

conformation of the oleate-bound HSA is the same as the equivalent defatted fraction. Thus both the binding of oleate and binding to the phenyl-Sepharose column appear to result in the same conformational change.

The rate of oleate binding, as measured by the reduction of acrylamide quenching, gives a result for the rate of reaction that is on the same order of magnitude as the result given by Bjerrum et al. (1995) for the reequilibration of the two fractions separated by HIC. This supports the above proposal that oleate binding and binding to the phenyl-Sepharose column result in the same conformational change. The identity of the conformational changes of the defatted HSA to the oleate-bound form may be the HSA-myristoylate structure reported by Curry et al. (1998). In the latter, rotations of HSA domains I and III appear to have taken place after the binding of the myristoylate.

In this study, the effects of oleate binding to HSA have been examined by a number of techniques. The results imply that large-scale structural changes in the albumin take place over a long time scale. The physiological manifestations of this behavior are likely to have some bearing on an understanding of the cellular selection of albumins (Wall et al., 1995) that are (or not) complexed to ligands such as oleate. Thus these phenomena may represent the molecular basis for the important function of the transport and targeting of ligands throughout the mammalian circulatory system.

We are grateful to Andaris Ltd. (Nottingham, England) for financial support and for providing samples of HSA for this work. We are also grateful to Drs. Roy Harris and David Coghlan of the same organization for helpful discussions. We also thank Dr. Stephen Curry and Prof. Nick Franks for helpful discussions.

REFERENCES

- Ameloot, L., H. Hendrickx, W. Herreman, H. Pottel, F. Van Cauwelaert, and W. Van Der Meer. 1984. Effect of orientational order on the decay of the fluorescence anisotropy in membrane suspensions—experimental verification on unilamellar vesicles and lipid alpha-lactalbumin complexes. *Biophys. J.* 46:525–539.
- Bain, A. J., J. Bryant, and R. J. Dean. 1998. Direct measurement of anisotropic probe motion in ordered systems. Proceedings of IQEC 1998, paper QWD2, OSA Technical Digest Series Vol. 7, 98–99.
- Bain, A. J., P. Chandna, and G. Butcher. 1996. Strong molecular alignment in anisotropic fluid media. *Chem. Phys. Lett.* 260:441–446.
- Bain, A. J., and A. J. McCaffery. 1984. Complete determination of the state multipoles of rotationally resolved polarized fluorescence using a single experimental geometry. *J. Chem. Phys.* 80:5883–5892.
- Bjerrum, O. J., M. J. Bjerrum, and N. H. H. Heegard. 1995. Electrophoretic and chromatographic differentiation of two forms of albumin in equilibrium at neutral pH—new screening techniques for determination of ligand binding to albumin. *Electrophoresis*. 16:1401–1407.
- Callis, P. R. 1997. 1L_a and 1L_b transitions of tryptophan: applications of theory and experimental observations to fluorescence of proteins. *Methods Enzymol.* 278:113–150.
- Carter, D. C., and J. Ho. 1994. Structure of serum albumin. *Adv. Protein Chem.* 45:153–203.
- Chen, R. F. 1967. Removal of fatty acids from serum albumin by charcoal treatment. *J. Biol. Chem.* 242:173–187.
- Curry, S., H. Mandelkow, P. Brick, and N. Franks. 1998. Crystal structure of human serum albumin complexed with fatty acids reveals an asymmetric distribution of binding sites. *Nature Struct. Biol.* 5:827–835.
- Dahms, T. E. S., K. J. Willis, and A. G. Szabo. 1995. Conformational heterogeneity of tryptophan in a protein crystal. *J. Am. Chem. Soc.* 117:2321–2326.
- Eftink, M. R., and C. A. Ghiron. 1976. Exposure of tryptophanyl residues in proteins. Quantitative determination by fluorescence quenching studies. *Biochemistry*. 15:672–680.
- Eftink, M. R., and C. A. Ghiron. 1977. Exposure of tryptophanyl residues and protein dynamics. *Biochemistry*. 16:5546–5551.
- Gentin, M., M. Vincent, J. Brochon, A. K. Livesey, N. Cittanova, and J. Gallay. 1990. Time-resolved fluorescence of the single tryptophan residue in rat α -fetoprotein and rat serum albumin: analysis by the maximum-entropy method. *Biochemistry*. 29:10405–10412.
- Gratton, E., J. R. Alcala, and G. Marriott. 1986. Rotations of tryptophan residues in proteins. *Biochem. Soc. Trans.* 14:835–838.
- Hansen, J. E., S. J. Rosenthal, and G. R. Flemming. 1992. Subpicosecond fluorescence depolarization studies of tryptophan and tryptophanyl residues of proteins. *J. Phys. Chem.* 96:3034–3040.
- Hochstrasser, R. M., and D. K. Negus. 1984. Picosecond fluorescence decay of tryptophans in myoglobin. *Proc. Natl. Acad. Sci. USA*. 81:4399–4403.
- Ichiye, T., and M. Karplus. 1983. Fluorescence depolarization of tryptophan residues in proteins—a molecular dynamics study. *Biochemistry*. 22:2884–2893.
- Janatova, J., J. K. Fuller, and M. J. Hunter. 1968. The heterogeneity of bovine albumin with respect to sulphhydryl and dimer content. *J. Biol. Chem.* 243:3612–3622.
- Janes, S. M., G. Holtom, P. Ascenzi, M. Brunori, and R. M. Hochstrasser. 1987. Fluorescence and energy transfer of tryptophans in *Aplysia* myoglobin. *Biophys. J.* 51:653–660.
- Kinosita, K., Jr., S. Kawato, and A. Ikegami. 1977. Theory of fluorescence polarisation decay in membranes. *Biophys. J.* 20:289–305.
- Lakowicz, J. R. 1986. Principles of Fluorescence Spectroscopy. Plenum Press, New York.
- Lakowicz, J. R., and I. Gryczynski. 1992. Tryptophan fluorescence intensity and anisotropy decays of HSA resulting from one-photon and two-photon excitation. *Biophys. Chem.* 45:1–6.
- Lakowicz, J. R., and G. Weber. 1973. Quenching of protein fluorescence by oxygen. Detection of structural fluctuations in proteins on the nanosecond time scale. *Biochemistry*. 12:4171–4179.
- Lehrer, S. S. 1971. Solute perturbation of HSA fluorescence by iodide. *Biophys. J.* 11:72a.
- Ludescher, R. D., J. J. Volwerk, G. H. de Haas, and B. S. Hudson. 1985. Complex photophysics of the single tryptophan of porcine pancreatic phospholipase-A-2, its zymogen, and an enzyme micelle complex. *Biochemistry*. 24:7240–7249.
- Munro, I., I. Pecht, and L. Stryer. 1979. Subnanosecond motions of tryptophan residues in proteins. *Proc. Natl. Acad. Sci. USA*. 76:56–60.
- Narazaki, R., T. Maruyama, and M. Otagiri. 1997. Probing the cysteine 34 residue in human serum albumin using fluorescence techniques. *Biochim. Biophys. Acta*. 1338:275–281.
- Nishimoto, E., S. Yamashita, A. G. Szabo, and T. Imoto. 1998. Internal motion of lysozyme studied by time-resolved fluorescence depolarisation of tryptophan residues. *Biochemistry*. 37:5599–5607.
- O'Connor, D. V., and D. Philips. 1984. Time Correlated Single Photon Counting. Academic Press, London.
- Peters, T. 1996. All About Albumin. Academic Press, London.
- Rose, H., M. Conventz, Y. Fischer, E. Jüngling, T. Hennecke, and H. Kammermeier. 1994. Long-chain fatty-acid binding to albumin—reevaluation with directly measured concentrations. *Biochim. Biophys. Acta*. 1215:321–326.
- Ross, J. B. A., K. W. Rousslang, and L. Brand. 1981a. Time-resolved fluorescence and anisotropy decay of the tryptophan in adrenocorticotropin-(1–24). *Biochemistry*. 20:4361–4369.
- Ross, J. B. A., C. J. Schmidt, and L. Brand. 1981b. Time-resolved fluorescence of the two tryptophans in horse liver alcohol dehydrogenase. *Biochemistry*. 20:4369–4377.
- Scheider, W. 1980. Ligand-independent activated state of serum albumin for fatty acid binding. *J. Phys. Chem.* 84:925–928.

- Soetewey, F., M. Rosseneu-Motreff, R. Lamote, and H. Peeters. 1972. Size and shape determination of native and defatted BSA monomers. *J. Biochem.* 71:705–710.
- Szabo, A. J., and D. M. Raynor. 1980. Fluorescence decay of tryptophan conformers in aqueous solutions. *J. Am. Chem. Soc.* 102:554–563.
- Valeur, B., and G. Weber. 1977. Resolution of the fluorescence excitation spectrum of indole into the 1L_a and 1L_b excitation bands. *Photochem. Photobiol.* 25:441–444.
- Wall, J., F. Ayoub, and P. O'Shea. 1995. Interactions of macromolecules with the mammalian cell surface. *J. Cell. Sci.* 108:2673–2682.
- Weiseger, R., J. Gollan, and R. Ockner. 1981. Receptor for albumin on the liver cell surface may mediate uptake of fatty acids and other albumin-bound substances. *Science*. 211:1048–1050.
- Willis, K. J., W. Neugebauer, M. Sikorska, and A. G. Szabo. 1994. Probing alpha-helical secondary structure at a specific site in model peptides via restriction of tryptophan side-chain rotamer conformation. *Biophys. J.* 66:1623–1630.
- Yamamoto, Y., and J. Tanaka. 1972. Polarised absorption spectra of crystals of indole and its related compounds. *Bull. Chem. Soc. Jpn.* 65:1362–1366.